A Two-Dimensional Cellular Automaton Model of Parasystole

MEGHA KODANCHA, DR. GIL BUB, KHADY DIAGNE, STEN KAJITANI

Abstract

Under normal cardiac conditions, the sinoatrial node is the pacemaking region which initiates depolarization in the heart; in parasystole, there also exists an ectopic pacemaker which may initiate depolarization waves. Parasystole is a form of arrhythmia caused by the influence of the secondary pacemaker on cardiac behaviour. Specifically, we consider cases of pure parasystole, where the two pacemakers are protected from each other. Previous theoretical models of pure parasystole consider the interaction of two pacemakers without incorporating physical space. The objective here is to create a simple, theoretical, two-dimensional model of pure parasystole where the distance between the pacemakers may be adjusted. A cellular automaton model was created using Python 3.8.3 and associated packages. The model was used to evaluate how changes in space influenced cell activation cycles and the number of intervening sinus beats (the number of times cells were activated by the sinus node versus the ectopic pacemaker). The model dynamics were further compared to experiments using optogenetic methods to stimulate a cardiac monolayer from two sites. This model provides insight into the physical dynamics of parasystole in its most basic form so that it may be built upon to eventually be used in a clinical context.

Introduction and Review of Literature

The function of the mammalian heart depends on its ability to propagate action potentials and contract synchronously. An action potential (AP) is a brief period of electrical depolarization followed by a brief period of electrical repolarization near the cellular membrane (Wei et al. 2020). Under normal physiological conditions, the sinoatrial (SA) node initiates cardiac depolarization waves to the rest of the heart (Alanís et al. 1958). As the wave propagates, the propagation speed slows down near the atrioventricular (AV) node to provide time for the atria to contract ahead of the ventricles. The AP depolarization typically lasts for 250 milliseconds and the absolute repolarization period lasts for 150 milliseconds, after which the cell is brought to rest to be excited again (Kléber & Rudy, 2004). The electrical impulse is coupled with a physical contraction, which allows the pumping of blood (Bers et al., 2002).

Parasystole is an arrhythmia where there exists a secondary pacemaker, along with the SA node, that may propagate AP waves itself. The influence of this secondary, otherwise known as ectopic, pacemaker on cardiac electrical properties can lead to arrhythmias and uneven heart contractions. Cardiac contractions from the SA node are known as sinus beats and contractions from the ectopic pacemaker are known as ectopic beats (Pick, 1953).

Parasystole was originally defined by GB Fleming (Fleming, 1912). According to Fleming, fusion beats are when both the SA node and ectopic pacemaker fire together, and the ectopic pacemaker is protected from depolarization by the sinus node (Pick, 1953). The protection of the ectopic focus is due to a surrounding region of tissue that tends to propagate waves in only one direction.

When two pacemakers can electronically influence each other, it is called modulated parasystole; when they are protected from each other, it is referred to as pure parasystole. Mathematical models of pure parasystole assume that there is no electronic influence between the pacemakers. In the theoretical

https://doi.org/10.33178.SMJ.2024.1.2

model by Glass et al. in 1986, the authors varied the ratios between the sinus pacemaker period (S) and the ectopic pacemaker period (E), and between S and the refractory period after a sinus beat (θ) (Glass et al., 1986). During each variation they recorded the number of intervening sinus beats (NIBs) between ectopic beats and proposed the following set of rules for pure parasystole at fixed E, S and θ values:

1. There are at most three different values for the NIBs.
2. One and only one of these NIBs is odd.
3. The sum of the two smaller values is one less than the largest value.

These results allowed the authors to predict the NIBs depending on the E/S and the θ/S ratios in a dimensionless environment (Fig 1).

A consideration not made in the paper above or other models of parasystole is the distance between the pacemaking regions, which is an important feature to study because it influences the timing of dynamics. If the distance between pacemaking sites varies, we would expect to see varying NIBs.

This project aims to display the dynamics in pure parasystole when the distance between the pacemakers can be controlled. We created a two-dimensional (2D) Cellular Automaton (CA) model to run simulations on and compared the outputs of the model to the results of optogenetic experiments and data collected by theoretical models. We hypothesized that there will be differences in parasystole dynamics when the distance between the pacemaking regions changes, and we worked towards quantifying this relationship.

A CA model is a common tool to estimate the propagation of AP in neurological and cardiac cells (Mordvintsev et al. 2020). Rules to creating 2D CA models of cardiac cells are laid out in Bub, et al. 1998 (Bub et al. 1998). The 2D CA model of parasystole is a continuation of the work started by Diagne 2020, which considers the dynamics of parasystole in a one-dimensional (1D) CA model (Diagne, 2020). The 1D model concluded that when modeling pure parasystole without interpolated beats, the three NIB rules from Glass et al. 1986 are upheld at any point in space. Additionally, the NIB triplet sequence changes as one moves spatially away from the ectopic pacemaker, mirroring the sequence seen when the refractory period increases in a dimensionless model. We believe that our 2D CA model would output NIB patterns similar to those seen in the 1D model and in the theoretical Glass 1986 model. A great advantage of 2D CA models is that their outputs can be directly compared to the outputs of optogenetic experiments that use myocyte plates.

Optogenetic techniques allow us to generate two interacting pacemakers where the distance between the pacemakers and their relative periods can be adjusted. By generating cardiac monolayers of neonatal mice myocytes and virally transfecting them to express light sensitive channels, the monolayers can be stimulated to propagate APs using patterned light (Burton et al. 2015). This method allows us to change the distance between pacemakers more easily than with electrical stimulations (Van Meerwijk et al. 1984). Furthermore, this technique is less damaging to the tissues and provides better fluorescent visuals (Sepúlveda, 2020). The results of such experiments can then be compared

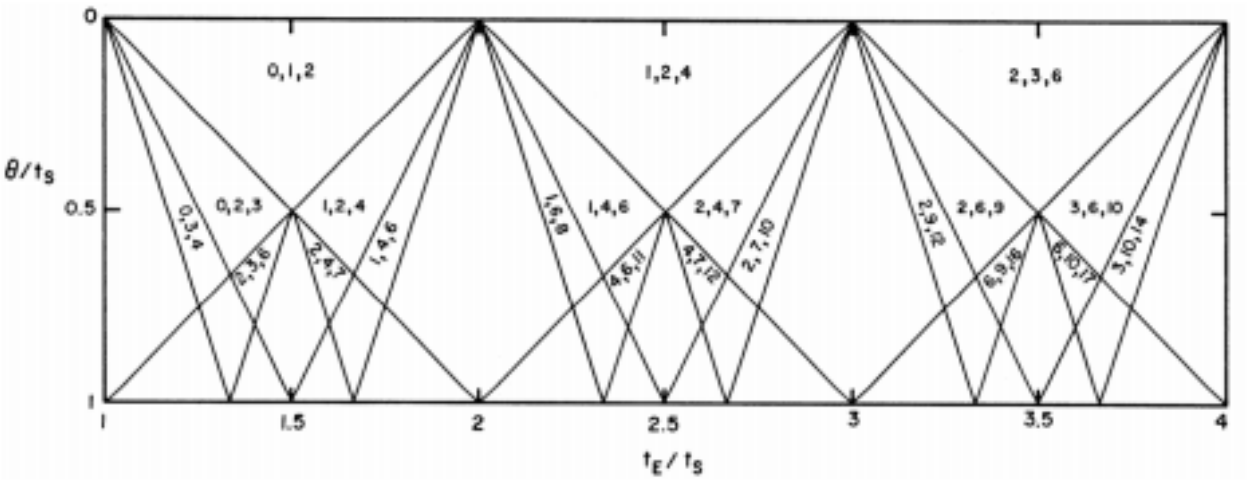

Figure 1: Allowed values of NIB depending on E/S and θ/S values. Farey diagrams of order 3. (from Glass et al. 1986)

to the results of the 2D CA simulations to ensure that the model accurately depicts cardiac behaviour.

'Simple' models of parasystole serve as a crucial foundation for comprehending arrhythmic patterns and advancing clinical interventions. These findings can pave the way for the refinement of more intricate models incorporating additional anatomical properties and parameters.

Methods and Materials

The 2D CA is run in the programming language Python 3.8.3. The Python libraries used are numpy (allows for creation and manipulation of multi-dimensional arrays), pandas (allows for large data manipulation and for creating and reading Excel files), and plotly (allows for production of interactive and high-quality graphs).

The Cellular Automaton (CA) is two-dimensional grid of discrete cells that are adjusted through time based on certain predetermined rules. Each cell in the model represents a space of 1 mm × 1 mm and each time step lasts either 1 ms or 2 ms (this will depend on what the model is representing and is explained further in the results section).

In the following work, we utilized videos of optogenetic experiments on myocyte plates that were obtained by other members of the lab (Sepúlveda, 2020).

Results

The original (first) CA model is created using methods from Bub et al. 1998 and Diagne 2020. The model consists of N × N cells where numerical states 1, 2, …, E are excitatory, E+1, E+2, …, E+R are refractory, and state 0 (also corresponding to state E+R+1) is inactive. Neighbours are the cells surrounding the cell of focus. The states are updated at every time step according to the following rules:

if $1 \leq state^t \leq E+R$:
    $state^{t+1} = state^t$
if $state^t = E+R+1$:
    $state^{t+1} = 0$

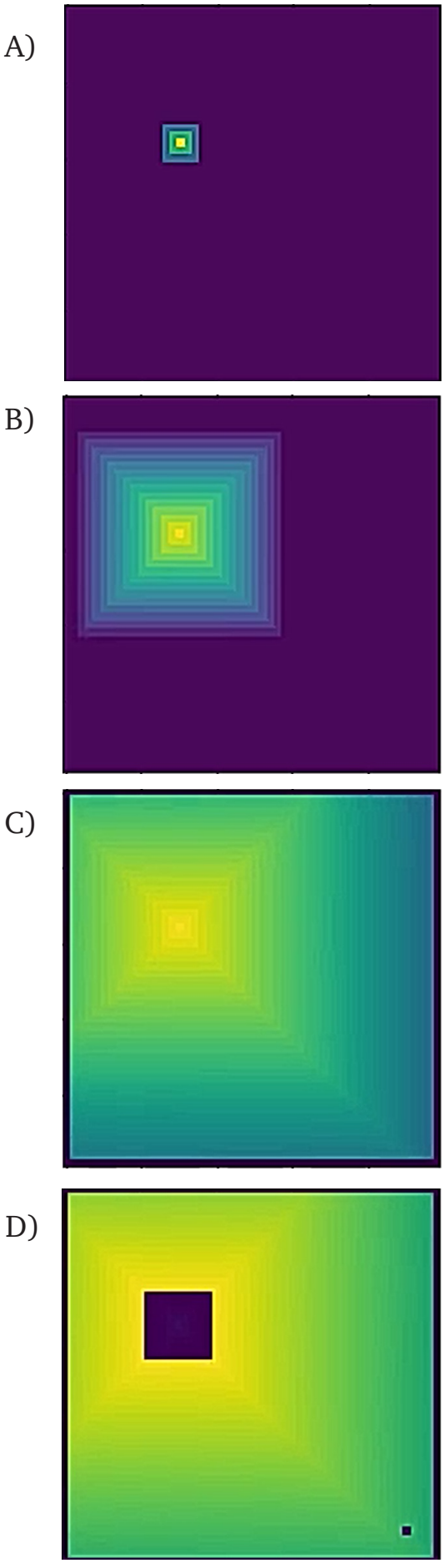

Figure 2: Images of Simulation taken with the first 2D CA Model. Parameters were ro = 50, co = 50, Period_PM1 = 160, t2 = 0, E = 90, R = 26, # neigh = 1. Sinus node was located at (18,13) and ectopic node was located at (45,45). The times taken from the video A) 1:21, B) 1:23, C) 1:31, and D) 1:37.

if $state^t = 0$:
    if $1 \leq$ neighbour $states^t \leq E$:
        $state^{t+1} = 1$
    else:
        $state^{t+1} = 0$

The neighbourhood of a cell may be the immediate cells surrounding it or can include further layers. The neighbour layers are defined in square formations. If any one of a cell's neighbours is active, the cell will become activated in the next time step. When running simulations with this model, the propagation waves appear 'square-like' and do not accurately depict cardiac behaviour (Fig 2).

The updated (second) CA model includes all the rules above except line (6) which is modified to incorporate an activation threshold and spatial heterogeneity. The modification to incorporate an activation threshold was adapted from Bub et al. 2002 (Bub et al. 2002). The model considers the number of excitatory neighbours over the total number of neighbouring cells, and if this exceeds a threshold value θ, the cell will be activated: θ is a fixed activation threshold value, typically varying between 0.20 – 0.50.

$$\frac{number\ of\ excitatory\ neighbours}{total\ number\ of\ neighbouring\ cells} \geq \theta$$

θ is a fixed activation threshold value, typically varying between 0.20 – 0.50.

We also introduce spatial heterogeneity to the second model by incorporating some randomness at the borders between influential neighbouring cells (ones that contribute more strongly to the activation of the cell) and non influential neighbouring cells. For two neighbouring cells with initial coordinates x0 and y0, the new coordinates would be x0 + x and y0 + y where x and y are randomly chosen as either –1 or 1. Based on the new coordinates, some cells immediately outside the borderline may become influential neighbours whereas some cells within the borderline may no longer be influential neighbours. When this adjustment is incorporated, the activation waves become more heterogeneous and similar to propagation waves seen in optogenetic experiments on myocyte cell plates.

The model also includes a tracker which evaluates if the cell has been activated by the ectopic or sinus pacemaker. This is used to evaluate the number of intervening beats each cell in the model experiences over time.

The input parameters of the model are:

- The number of rows in the grid (ro)
- The number of columns in the grid (co)
- The number of time steps (time_steps)
- The x and y coordinates of the sinus node (PM1x, PM1y)
- The activation period of the sinus node (Period_PM1)
- The x and y coordinates of the ectopic node (PM2x, PM2y)
- The activation period of the ectopic node (Period_PM2)
- The delay time before the ectopic node begins propagating waves (t2)
- The cell activation period of each cell (E)
- The refractory period of each cell (R)
- The number of layers of influential neighbours (# neigh)
- The activation threshold ()

Two sets of parameter choices were taken to evaluate parasystole dynamics. In the first, we took parameters that we would see on the myocyte plates. In this case, each time step is of 2 ms, and each cell represents a space of 1 mm × 1 mm. For the simulations we set ro = 100, co = 100, Period_PM1 = 160, t2 = 0, E = 90, R = 26, # neigh = 2, θ = 0.4; we then vary PM1x, PM1y, PM2x, and PM2y throughout the simulation. The value of Period_PM2 is varied with each simulation to determine how its influence will affect the NIBs along space; the ratio of the ectopic pacemaker period (Period_PM2) to the sinus pacemaker period (Period_PM1) is typically set between 1.0 – 2.0. The results from the CA simulations were then qualitatively compared to videos of myocyte plate propagations.

The visualizations created by the 2D CA model do mimic myocyte behaviour (Fig 3). We conclude from the simulations that the NIBs for the cells in the 2D CA do vary in space. These dynamics can be depicted visually, where each colour is associated with a different list of NIBs (Fig 4) (Supplementary 1). In

Figure 3: Images of Simulation taken with the second 2D CA Model. Parameters were ro = 100, co = 100, Period_PM1 = 160, Period_PM2 – 240, t2 = 0, E = 90, R = 26, # neigh = 2, θ = 0.4. Sinus node was located around (10,10) and ectopic node was located around (76,76). The times taken from the video A) 1:21, B) 1:23, C) 1:31, and D) 1:37.

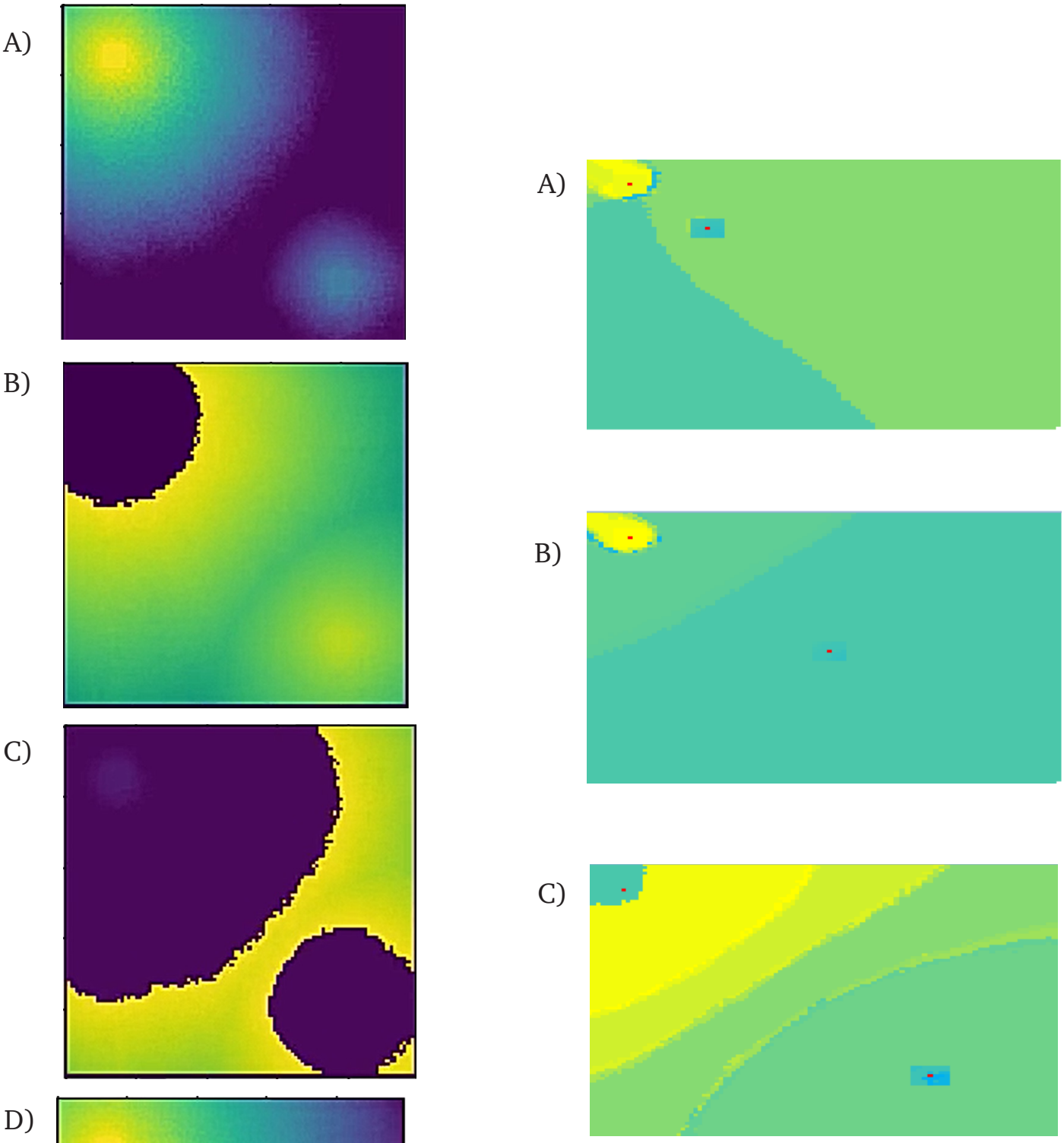

Figure 4: The NIBs data collected for simulations taken with the second 2D CA Model. Parameters were ro = 100, co = 100, Period_PM1 = 160, Period_PM2 = 240, t2 = 0, E = 90, R = 26 # neigh = 2, θ = 0.4. The sinus node was in position (10,10) and the ectopic node (shown in red) was in position: A) (26,26), B) (51,51), and C) (76,76). Each colour is associated to a different list of NIBs described in Figure 5.

these visualizations the ratio of the ectopic pacemaker period (Period_PM2) to the sinus pacemaker period (Period_PM1) is 1.5. We can also see the dividing lines between varying NIBs values. For example, the dividing line shifts dramatically from the first and second image (Fig 4.A and 4.B, respectively). This indicates that there is a critical point during which the ectopic node is between coordinates (26, 26) and (51, 51) when this dramatic shift occurs. This is an aspect that needs to be further explored in future simulations. Moreover, most of these cells typically experience more than three NIBs, meaning that they do not follow the rules set by Glass, et al 1986 (Supplementary 1). This may occur because the model does not follow the longer refractory periods found within in vivo cardiac tissue. We therefore decided to investigate a second set of parameters.

In our second set of simulations, we consider parameters that mimic the properties of cardiac cells which allow the whole heart to be activated before the beginning of a new wave of depolarization. In this case, each time step is set to 1 ms, and each cell represents a space of 1 mm × 1 mm. These simulations are compared with those in the 1D model and in the theoretical model suggested by Glass, et al 1986. We set ro = 100, co = 100, Period_PM1 = 800, t2 = 0, E = 100, R = 220, # neigh = 2, = 0.4; we then vary PM1x, PM1y, PM2x, and PM2y throughout the simulation. The value of Period_PM2 is varied with each simulation, like in the first simulation. Here the data suggests that the NIBs are not affected by the space between the nodes and for the most part, the ectopic node's dynamics are covered by the sinus node propagation. Only when the ratio between the periods is between 1.0 – 1.2 does one see small variations in the NIBs as a function of space. In these cases, the NIBs are (0, 1, 2) or (0, 1) (Fig 5), following the rules set by Glass, et al 1986 and the 1D model. Additionally, we observe that the dividing line between the different NIBs shifts by the same distance as the ectopic node does in each simulation. However, no other data matches the theoretical model, and when the ratio between periods was set above 1.5, there were no NIBs present.

Results

The data suggests that NIBs in cardiac cells are influenced by the space between the pacemaking nodes in a 2D CA Model. The simulation outcome supports the results found by Glass, et al 1986 and Diagne, 2020 when the ectopic pacemaker has a period 1.0 – 1.2 times that of the sinus pacemaker, but not otherwise. We have further shown that varying ratios for the periods of the two pacemakers in physiological ranges can also influence the overall dynamics in parasystole.

Currently, one of the model's limitations is its lack of a third dimension, meaning that it cannot entirely depict the dynamics of a 3D mammalian heart. However, we would expect to observe similar dynamics in a 3D model as we would in our 2D model. Another limitation is that the data is discrete in time, which limits the temporal resolution of the parasystole dynamics being visualized.

To advance the project and address the aforementioned limitations, we aim to develop a 3D model of pure parasystole to evaluate NIBs in three dimensions and compare this to the findings in 2D. We also plan on incorporating methods to represent time as a continuous, as opposed to discrete, variable so that it is more representative of live tissue (Ito et al. 1991). Furthermore, we aim to provide more in-depth quantitative explanations for how the space between pacemakers influences dynamics.

Conclusion

One of the original purposes of the project was to create a 2D CA model of parasystole that could be comparable to myocyte plates that have been stimulated using optogenetics. We wanted to create a model that views the impact of space upon parasystole since this is a less explored topic when determining dynamics like NIBs. Through progressive treatment, the 2D CA Model currently estimates dynamics very similar to those seen in myocyte plate recordings.

Ultimately, this project aims to quantify the dynamics observed in pure parasystole for prospective clinical applications. Although the model we propose cannot be used clinically, it may serve as a basis to build a 3D model of cardiac tissue. By beginning to understand the influence of space on parasystole, we can develop a better understanding of the physiology of parasystole.

Acknowledgments

I want to thank Dr. Gil Bub, Khady Diagne, José Miguel Romero Sepúlveda, and Thomas Michael Bury

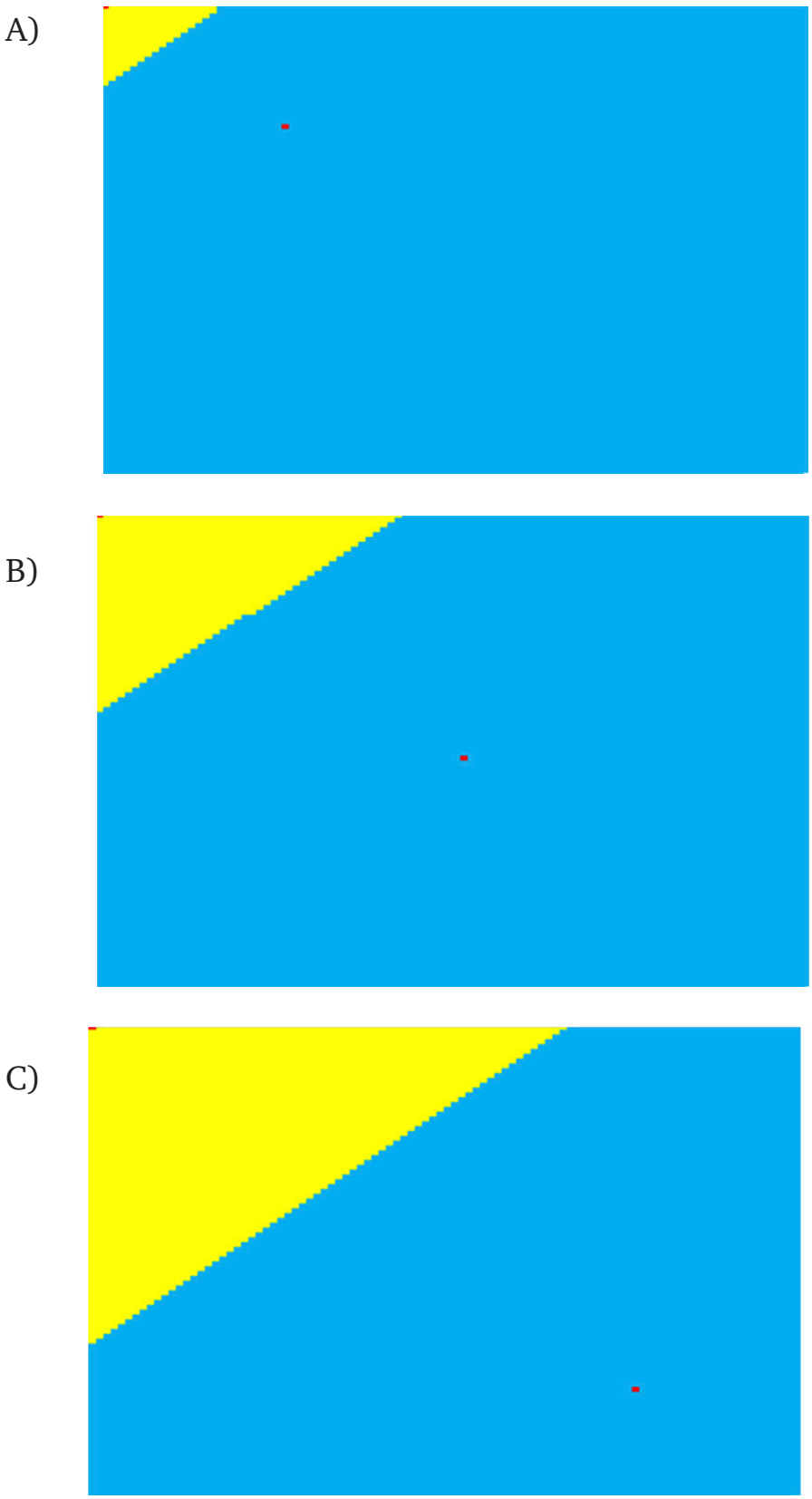

Figure 5: The NIBs data collected for simulations taken with the second 2D CA Model. Parameters were ro = 100, co = 100, Period_PM1 = 800, Period_PM2 = 960, t2 = 0, E = 100, R = 220, # neigh = 2, θ = 0.4. The sinus node was in position (10,10) and the ectopic node (shown in red) was in position: A) (26,26), B) (51,51), and C) (76,76). Yellow represents NIBs = (0,1) and blue represents NIBs = (0,1,2).

References

1. Alanís, J., González, H., & López, E. (1958). The electrical activity of the bundle of His. The Journal of physiology, 142(1), 127-140.
2. Bers, D. M. (2002). Cardiac excitation–contraction coupling. Nature, 415(6868), 198-205.
3. Bub, G., Glass, L., Publicover, N. G., & Shrier, A. (1998). Bursting calcium rotors in cultured cardiac myocyte monolayers. Proceedings of the National Academy of Sciences, 95(17), 10283-10287. doi:10.1073/pnas.95.17.10283
4. Bub, G. Ito, H. Glass, L. (1991) Spiral Breakup in a New Model of Discrete Excitable Media. Physical Review Letters, vol. 66, no. 5, doi:10.1103/physrevlett.88.058101.
5. Burton, R. A., Klimas, A., Ambrosi, C. M., Tomek, J., Corbett, A., Entcheva, E., & Bub, G. (2015). Optical control of excitation waves in cardiac tissue. Nature photonics, 9(12), 813-816.
6. Fleming, G. B. (1912). Triple rhythm of the heart due to ventricular extrasystoles. QJ Med, 5, 318-326
7. Glass, L., Goldberger, A. L., & Belair, J. (1986). Dynamics of pure parasystole. American Journal of Physiology-Heart and Circulatory Physiology, 251(4), H841-H847
8. Ito, H. & Glass, L. (1991) Spiral breakup in a new model of discrete excitable media. Physical Review Letters 66, 671–674
9. Kléber, A. G., & Rudy, Y. (2004). Basic mechanisms of cardiac impulse propagation and associated arrhythmias. Physiological reviews, 84(2), 431-488.
10. Mordvintsev, A., Randazzo, E., Niklasson, E. & Levin, M. (2020). Growing Neural Cellular Automata. Distill. [Internet]
11. Pick, A. (1953). Parasystole. Circulation, 8(2), 243-252. doi:10.1161/01.cir.8.2.243
12. VanMeerwijk, W. P., Debruin, G., Ginneken, C. G., Vanhartevelt, J., Jongsma, H. J., Kruyt, E. W., . . . Ypey, D. L. (1984). Phase resetting properties of cardiac pacemaker cells. Journal of General Physiology, 83(4), 613-629. doi:10.1085/jgp.83.4.613
13. Wei X, Yohannan S, Richards JR. (2020). Physiology, Cardiac Repolarization Dispersion and Reserve. StatPearls [Internet]
14. Unpublished Thesis: Diagne, K. (2020). Discrete and Continuous One-Dimensional Models of Parasystole.
15. Unpublished Thesis: Sepúlveda, J. M. R. (2020). Optically Induced Heterogeneities in Cardiac Tissue.

Supplementary

1	[0, 1, 2, 3]	31	[11, 0, 3, 19, 15, 6, 4]	61	[12, 47, 11]
2	[0, 1, 2, 4, 3]	32	[11, 0, 3, 19, 15, 7, 2, 4]	62	[12, 47, 2, 0, 3]
3	[0, 1, 2]	33	[11, 0, 3, 19, 15, 7, 6, 4]	63	[12, 6, 4, 13, 7, 2, 8]
4	[0, 1, 3, 2, 4]	34	[11, 35]	64	[12, 6, 4, 2, 0, 17, 13, 7]
5	[0, 1, 3, 2, 5]	35	[12, 1, 9, 2, 0, 5, 24]	65	[15, 14, 47]
6	[0, 1, 3, 2]	36	[12, 11, 14, 8]	66	[16, 15, 47]
7	[0, 1]	37	[12, 11, 18, 6, 9, 2, 5]	67	[16, 15, 48]
8	[0, 10, 2, 13, 3, 5, 4, 1]	38	[12, 11, 25, 1, 7, 2, 8]	68	[16, 15, 49]
9	[0, 10, 2, 3, 9, 4, 1, 6]	39	[12, 11, 35, 2, 3]	69	[16, 15, 50]
10	[0, 2, 1, 3]	40	[12, 11, 35, 2, 8]	70	[16, 50]
11	[0, 2, 1, 4, 3]	41	[12, 11, 35, 3, 7]	71	[17, 16, 50]
12	[0, 2, 1]	42	[12, 11, 35]	72	[18, 16, 52, 17]
13	[0, 2, 3, 1]	43	[12, 2, 0, 4, 11, 3, 6]	73	[18, 17, 53]
14	[0, 2, 3, 4, 1]	44	[12, 2, 0, 7, 11, 15, 4, 3]	74	[2, 0, 1, 3]
15	[0, 2, 4, 1, 6, 3, 5]	45	[12, 2, 4, 0, 18, 5, 7, 3]	75	[2, 0, 3, 1, 6, 7]
16	[0, 2, 4, 7, 1, 3]	46	[12, 2, 8, 6, 9, 11]	76	[2, 7, 1, 0, 4, 9, 3]
17	[0, 2, 8, 1, 3]	47	[12, 23, 11]	77	[2, 7, 1, 0, 6, 5, 4]
18	[0, 2, 8, 3, 7, 11, 12, 6, 1]	48	[12, 23, 15, 7, 11]	78	[3, 0, 1, 2, 6, 4]
19	[0, 2, 8, 7, 11, 3, 4, 6, 1]	49	[12, 23, 15, 7, 6, 4]	79	[3, 2, 0, 1]
20	[0, 5, 4, 2, 10, 9, 1, 3]	50	[12, 23, 6, 4]	80	[3, 2, 1, 0, 5, 6]
21	[0, 5, 4, 2, 13, 3, 9]	51	[12, 27, 10, 0, 7, 3]	81	[3, 7, 0, 2, 8]
22	[0, 5, 4, 2, 3, 1]	52	[12, 27, 19, 11]	82	[3, 8, 11, 25, 9]
23	[0, 5, 4, 2, 6, 3, 9, 7]	53	[12, 3, 7, 11, 15, 6, 0, 2, 1]	83	[3, 8, 2, 7, 0, 1, 6, 4, 5]
24	[0, 9, 2, 7, 5, 1, 4, 3]	54	[12, 3, 7, 11, 23]	84	[4, 7, 3, 6, 0, 2, 9, 8]
25	[10, 1, 11, 34, 0, 6]	55	[12, 3, 7, 2, 11, 6, 0, 1]	85	[6, 0, 4, 1, 3, 9, 8, 2]
26	[11, 0, 1, 43, 3, 7]	56	[12, 3, 7, 2, 32, 4]	86	[6, 5, 11, 1, 0, 7, 10, 4, 2]
27	[11, 0, 2, 13, 5, 3]	57	[12, 3, 7, 25, 1, 6, 0, 2, 4]	87	[6, 5, 3, 2, 4, 0, 1]
28	[11, 0, 2, 19, 15, 7, 3, 4]	58	[12, 3, 7, 35, 11]	88	[7, 2, 1, 3, 0, 10, 4]
29	[11, 0, 23, 15, 6, 2, 3, 4]	59	[12, 38, 7, 0, 11]		
30	[11, 0, 23, 15, 7, 6, 4]	60	[12, 39, 7, 6, 4]		

Supplementary 1 A: The NIBs data collected for simulations taken with the second 2D CA Model, associated to Fig 4 A. Shows the list of NIBs for each colour in Fig 4 A. Parameters were ro = 100, co = 100, Period_PM1 = 160, Period_PM2 = 240, t2 = 0, E = 90, R = 26 # neigh = 2, θ = 0.4. The sinus node was in position (10,10) and the ectopic node was in position (26,26)

1	[0, 1]	31	[1, 3, 0, 2, 4]	61	[27, 33, 0]
2	[0, 2, 1, 3, 4]	32	[1, 3, 10, 2, 0, 9, 4]	62	[27, 34]
3	[0, 2, 1, 3]	33	[1, 3, 14, 0, 4, 8, 5, 7, 2]	63	[36, 48]
4	[0, 2, 1, 4, 3]	34	[1, 3, 2, 0, 4, 5]	64	[37, 48]
5	[0, 2, 1]	35	[1, 3, 2, 0, 4, 6]	65	[37, 49]
6	[0, 2, 3, 1]	36	[1, 3, 2, 0, 4]	66	[38, 49]
7	[0, 2, 6, 1, 3, 4]	37	[1, 5, 0, 6, 3, 2, 4]	67	[38, 50]
8	[0, 2, 6, 1, 3]	38	[1, 6, 0, 2, 3, 4, 7]	68	[39, 49]
9	[0, 3, 1, 2]	39	[1, 6, 11, 2, 0, 3, 5, 10]	69	[39, 50]
10	[0, 3, 1, 5, 2, 4]	40	[1, 6, 11, 2, 0, 3, 5, 4]	70	[40, 51]
11	[0, 3, 2, 1, 4, 5]	41	[1, 6, 7, 3, 5, 0, 10]	71	[5, 10, 2, 4, 1, 0, 3, 17]
12	[0, 3, 2, 1, 4, 6]	42	[1, 6, 7, 3, 5, 0, 2, 4]	72	[5, 13, 6, 0, 14, 2, 4, 3]
13	[0, 3, 2, 1, 4]	43	[1, 9, 3, 8, 0, 11, 5, 4]	73	[5, 18, 1, 0, 21, 8, 2]
14	[0, 3, 2, 1]	44	[16, 9, 0, 4, 8]	74	[5, 20, 0, 14, 1, 4, 3, 2]
15	[0, 3, 2, 8, 1, 5]	45	[24, 1, 0, 21, 8, 2]	75	[5, 20, 0, 21, 9, 2]
16	[0, 4, 1, 3, 2]	46	[24, 1, 0, 3, 17, 9]	76	[5, 3, 0, 2, 4, 1, 13]
17	[0, 4, 2, 3, 1, 6]	47	[24, 1, 0, 4, 3, 23, 2]	77	[5, 3, 1, 0, 2]
18	[0, 5, 1, 2]	48	[26, 0, 2, 28]	78	[5, 3, 2, 0, 4, 1, 8]
19	[0, 5, 1, 8, 2, 6, 3]	49	[26, 0, 22, 9, 3]	79	[5, 3, 4, 1, 0, 17, 2]
20	[0, 6, 1, 7, 3, 2, 5]	50	[26, 0, 22, 9]	80	[5, 3, 4, 1, 0, 2, 7]
21	[0, 6, 3, 1, 2, 4, 5, 7]	51	[26, 0, 27, 4]	81	[5, 3, 8, 1, 0, 17, 2]
22	[0, 6, 3, 1, 2, 4]	52	[26, 0, 3, 28, 4]	82	[5, 9, 3, 4, 1, 0, 10, 8, 2]
23	[0, 6, 3, 5, 4, 1]	53	[26, 0, 3, 28]	83	[7, 16, 1, 0, 4, 8, 3, 9]
24	[1, 14, 3, 5, 0, 10, 4]	54	[26, 0, 32, 4]	84	[8, 0, 1, 3, 2]
25	[1, 14, 3, 5, 0, 12, 10]	55	[26, 0, 32]	85	[9, 16, 0, 2, 18, 10]
26	[1, 2, 0, 3, 6, 10]	56	[26, 0, 33]	86	[9, 16, 0, 4, 27]
27	[1, 24, 0, 4, 16, 10]	57	[26, 0, 34]	87	[9, 6, 0, 11, 4, 3, 2]
28	[1, 24, 0, 4, 5, 10, 7]	58	[26, 0, 4, 16, 10]		
29	[1, 24, 0, 4, 6, 2, 17]	59	[26, 0, 4, 27]		
30	[1, 24, 0, 8, 2, 6, 9, 3]	60	[26, 0, 6, 8, 16, 7]		

Supplementary 1 B: The NIBs data collected for simulations taken with the second 2D CA Model, associated to Fig 4 B. Shows the list of NIBs for each colour in Fig 4 B. Parameters were ro = 100, co = 100, Period_PM1 = 160, Period_PM2 = 240, t2 = 0, E = 90, R = 26 # neigh = 2, θ = 0.4. The sinus node was in position (10,10) and the ectopic node was in position (51,51)

1	[0, 1, 2]
2	[0, 1]
3	[0, 2, 1]
4	[0, 2, 3]
5	[0, 2]
6	[0, 3, 1, 4]
7	[0, 3, 1]
8	[0, 3, 2]
9	[0, 3, 4, 1]
10	[0, 3, 4]
11	[0, 3]
12	[0, 4, 1, 3]
13	[0, 4, 1]
14	[0, 4, 3, 1]
15	[0, 4, 3]
16	[0]
17	[1, 4, 5]
18	[1, 4]
19	[1, 5, 2]
20	[1, 5, 4]
21	[1, 5, 6, 2]
22	[1, 5]

Supplementary 1 C: The NIBs data collected for simulations taken with the second 2D CA Model, associated to Fig 4 C. Shows the list of NIBs for each colour in Fig 4 C. Parameters were ro = 100, co = 100, Period_PM1 = 160, Period_PM2 = 240, t2 = 0, E = 90, R = 26 # neigh = 2, θ = 0.4. The sinus node was in position (10,10) and the ectopic node was in position (76,76)